VK1^{TM} - A next-generation Airborne Gravity Gradiometer

Theo Aravanis*
Rio Tinto Exploration
Melbourne, VIC
theo.aravanis@riotinto.com

Jon Chen
UWA
Perth, WA
jon.chen@uwa.edu.au

Martin Fuechsle
UWA
Perth, WA
martin.fuechsle@uwa.edu.au

Mark Grujic
Rio Tinto Exploration
Perth, WA
mark.grujic@riotinto.com

Paul Johnston
UWA
Perth, WA
paul.johnston@uwa.edu.au

Yitping Kok
UWA
Perth, WA
yitping.kok@uwa.edu.au

Rhet Magaraggia
UWA
Perth, WA
rhet.magaraggia@uwa.edu.au

Anthony Mann
UWA
Perth, WA
anthony.mann@uwa.edu.au

Laurence Mann
UWA
Perth, WA
laurence.mann@uwa.edu.au

Stephen McIntosh
Rio Tinto Exploration
Melbourne, VIC
stephen.mcintosh@riotinto.com

Gerard Rheinberger
Rio Tinto Exploration
Brisbane, QLD
gerard.rheinberger@riotinto.com

David Saxey
Curtin University
Perth, WA
david.saxey@curtin.edu.au

Mark Smalley
UWA
Perth, WA
mark.smalley@uwa.edu.au

Frank van Kann
Rio Tinto Exploration
Perth, WA
frank.vankann@riotinto.com

Grant Walker
Rio Tinto Exploration
Perth, WA
grant.walker@riotinto.com

John Winterflood
UWA
Perth, WA
john.winterflood@uwa.edu.au

SUMMARY

The minerals exploration industry's demand for a highly precise airborne gravity gradiometer has driven development of the VK1^{TM} Airborne Gravity Gradiometer, a collaborative effort by Rio Tinto and the University of Western Australia. VK1^{TM} aims to provide gravity gradient data with lower uncertainty and higher spatial resolution than current commercial systems.

In the recent years of VK1^{TM} development, there have been significant improvements in hardware, signal processing and data processing which have combined to result in a complete AGG system that is approaching competitive survey-ready status. This paper focuses on recent improvements. Milestone-achieving data from recent lab-based and moving-platform trials will be presented and discussed, along with details of some advanced data processing techniques that are required to make the most use of the data.

Key words: Airborne Gravity Gradiometry, Gravimetry

INTRODUCTION

Unlike magnetic methods, where the precision and resolution of airborne data can approach that of ground data, airborne gravity has not yet been able to reproduce the same level of interpretable information as from a detailed ground gravity survey.

The gradient of the gravity field can be directly or indirectly measured in an airborne setting (Lee, 2001). The gravity gradient of a density anomaly is inversely related with the cube of the distance between the sensor and the anomaly (Hammond and Murphy, 2003). This results in Airborne Gravity Gradiometry (AGG) data more closely reflecting changes in near-surface density variations, while signals from deeper sources are attenuated. This is favourable in the minerals exploration application, where near surface variations in densities are of interest to geoscientists. While recent advances in commercially available AGG technology and processing (Christensen, 2013) have been made, many situations exist where benefit would be added with the availability of a highly-precise AGG instrument. Furthering understanding of small-scale structural features, paleochannel characteristics, hydrothermal alteration zonation and direct detection (e.g. kimberlites) are examples of situations where increased spatial resolution and reduced data uncertainty would provide value. With this in mind, Rio Tinto has pursued development of the VK1^{TM} AGG instrument.

In preparation for survey-quality test flights at the RJ Smith Airborne Gravity Gradiometry Test Range at Kauring, Western Australia, VK1^{TM} has undergone extensive laboratory testing on a 6-axis flight simulator, as well as ground-based moving-platform field trials. These tests indicate that VK1^{TM} gravity gradient data quality is competitive with leading existing AGG systems, while concurrently being able to deliver data at higher frequencies. Lab-based flight simulation tests have achieved noise levels of 15.2 Eö in a 0.5 Hz frequency bandwidth (~60 milli g turbulence), while field tests in a closed van have achieved levels of 25 Eö in the same bandwidth. Whilst every care has been made to ensure the noise values quote here are correct at the time of writing, calibration of the instruments is based on laboratory measurements which is incapable of fully replicating the full suite of low frequencies expected in flight conditions. Therefore the values quoted here need to be categorically confirmed in dynamic tests.

In addition, all reported noise figures describe the equivalent vertical gravity gradient (Gzz), although VK1 observes a combination of the horizontal and vertical gravity gradients (detailed further in this abstract). This distinction is important, as previous publications (e.g. Dransfield et al. 2010) report the observed gravity gradient within a frequency bandwidth without a clear definition of the relationship between the observed components of gravity gradient and the more interpretable vertical gravity gradient, Gzz.

HARDWARE

In the laboratory, VK1™ is tested on a six-axis hexapod flight simulator. Linear and angular acceleration data previously recorded on an IMU from low-level flights over the R J Smith AGG test range are used to simulate realistic survey conditions. Whilst all three linear and all three angular accelerations are simulated, the principle component of the turbulence is vertical linear acceleration. A power spectrum of this component for four consecutive flight lines is seen in Figure 1, from 0.01 Hz to 100 Hz. The restricted size of a laboratory requires a reduction of linear acceleration at low frequency (<0.1 Hz) and necessitates further testing in an enclosed vehicle before the instrument is ready to test in an aircraft.

The recorded signal undergoes significant post-processing to yield a gravity gradient that is free from aircraft motion and other non-geological factors. These other factors can be as many as 7 orders of magnitude larger than the desired geophysical response. An accurate gravity gradient model of the flight simulator surroundings is known. Once this model is accounted for in the post-processed signal, the residual gravity gradient is an indication of instrument noise. The noise profiles for four consecutive synthetic flight lines are shown in Figure 2, with a 0.5 Hz VK1™ survey bandwidth as well as a more common industry standard 0.2 Hz bandwidth. The Gzz-equivalent noise was observed to be 15.2 Eö in the 0.5 Eö bandwidth, and 12.3 Eö in the 0.2 Hz bandwidth. For reference, VK1 will initially measure an independent value of the gravity gradient at 1 second intervals, thus the highest measurable frequency will be 0.5 Hz, or a wavelength of approximately 120 m in normal survey conditions.

After successfully demonstrating stability and acceptable data quality in the flight simulations, the VK1™ instrument was mounted in an enclosed vehicle and tested in a field environment. The vehicle was repeatedly driven at approximately 25 km/h on a relatively flat, north-south section of a quiet road near the University of Western Australia, with regions of varying road-side topography on the western flank and flat to the east. Figure 3 shows the processed gravity gradient for four test runs along the same section of the road. The north-heading and south-heading sections are coloured differently to emphasise the repeatability of the observations in each direction. The difference in magnitude of several of the anomalies when heading north and south is due to driving on the left (closer to the hills driving north). The spatially-located gravity gradient can be seen in Figure 4, where several key geophysical responses are highlighted.

The gravity gradient signal in Figures 3 and 4 includes the geophysical responses of topography and cultural variations, un-modelled aspects due to the motion of the vehicle, and instrument noise. Given these factors, an estimate of instrument noise is not immediately clear. However, the standard deviation of the total observed gravity gradient was 25 Eö in the 0.5 Hz bandwidth.

At the heart of the VK1 instrument is a pair of balanced bars, oriented orthogonal to each other. The bars are aligned in the vertical plane but are free to be oriented in any horizontal direction by the operator. Therefore VK1™ is sensitive to both the vertical gravity gradient and the gravity gradient along some fixed definable horizontal heading. In the data shown in Figures 3 and 4, the instrument horizontal sensitive axis was not chosen to maximise the response of the topographic and cultural features, leading to a lower than optimal signal-to-noise ratio.

In these vehicle tests, the horizontal gravity gradient due to topographic variations is larger than the corresponding vertical gravity gradient. As VK1™ measures the difference between the vertical and horizontal gravity gradients, road-side topographic highs result in observed gravity gradient lows, as highlighted at points 'A' and 'B' in Figure 4. The same is true then the distance between the sensor and the road-side topography is reduced. As seen in Figure 4, the gravity gradient is generally larger on the side of the road closer to the topographic variations. The influences of some un-modelled aspects of the instrument are apparent, as suggested by the apparent gravity gradient low 'C' in Figure 3. This apparent low is coincident with a chicane on the road, as seen in Figure 4.

DATA PROCESSING

AGG datasets are processed with a range of assumptions that are valid within the data's uncertainty. Given the high-precision goal of the VK1™ system, some of these assumptions that held for current systems are no longer valid. One such assumption is that it is sufficient to calculate the gravity gradient of forward and inverse density models at discrete locations in space, corresponding to the locations of the delivered data.

However, delivered gravity gradient data are representative of the gravity gradient along the flight path within some time frame either side of the delivered location. To provide the best data for interpretation, forward and inverse models should be treated in the same manner; the modelled value at each data point should be representative of the response along the flight path within the same time frames as the observed data. This process of arriving at a representative value within a timeframe along the flight path will be referred to as spatial averaging.

Applied to terrain corrections, the necessity to apply spatial averaging is emphasised. Terrain often has a high magnitude and short wavelength gravity gradient response due to the large density contrast between ground and air, and the proximity of the ground to the aircraft. Because of this, and given that the effect of spatial averaging is greatest when the observed signal changes most along the flight path, spatial averaging has become part of the standard VK1™ data processing workflow, to maintain sub-Eö uncertainty. To demonstrate the significance of spatial averaging, an example of a simulated survey over the Central Andes is shown. The survey was designed with 100 m spaced, north-south lines with a 80 m nominal terrain clearance. The ground was modelled as a homogenous earth with no density variations. Applying a terrain correction to the data should therefore yield a zero terrain corrected anomaly. However, when a standard terrain correction (calculated at discrete points) is applied to the realistic observed data (that has been continually acquiring along the flight path), the effect of not applying spatial averaging is severe (standard deviation of 6 Eö, peak-to-peak errors of 80 Eö), as seen in Figure 5.

CONCLUSIONS

The Rio Tinto and University of Western Australia jointly developed VK1™ airborne gravity gradiometer has been continually and significantly improved in recent years. Laboratory and ground-based trials have confirmed the suitability of the technology, with current noise levels of 15.2 Eö in a 0.5 Hz bandwidth in lab-based flight simulations. Final moving-platform tests, including on a typical geophysical survey aircraft, are ongoing ahead of deployment in a survey role. The instrument is in a phase of rapid and constant improvement on the hardware, processing and software fronts, and well on the path to deliver 1 Eö/√Hz AGG data.

ACKNOWLEDGMENTS

The authors would like to thank the entire VK1™ team, past and present, for their dedication and perseverance. Likewise, we acknowledge Rio Tinto and the University of Western Australia for their support and foresight to push the boundaries of airborne geophysics.

REFERENCES

Christensen, A.N., Dransfield, M.H. and Van Galder, C., 2015, Noise and repeatability of airborne gravity gradiometry, First Break, Vol 33, No 4, 55 - 63

Dransfield, M.H., Le Roux, T. and Burrows, D., 2010, Airborne gravimetry and gravity gradiometry at Fugro Airborne Surveys, Airborne Gravity 2010, Abstracts from the ASEG-PESA Airborne Gravity 2010 Workshop, 49-57.

Hammond, S., and Murphy, C.A., 2003, Air-FTG™: Bell Geospace's gravity gradiometer – a description and case study, ASEG Preview, 105, 24-26.

Lee, J.B., 2001, FALCON gravity gradiometer technology, Exploration Geophysics, 32(3/4), 247-250.

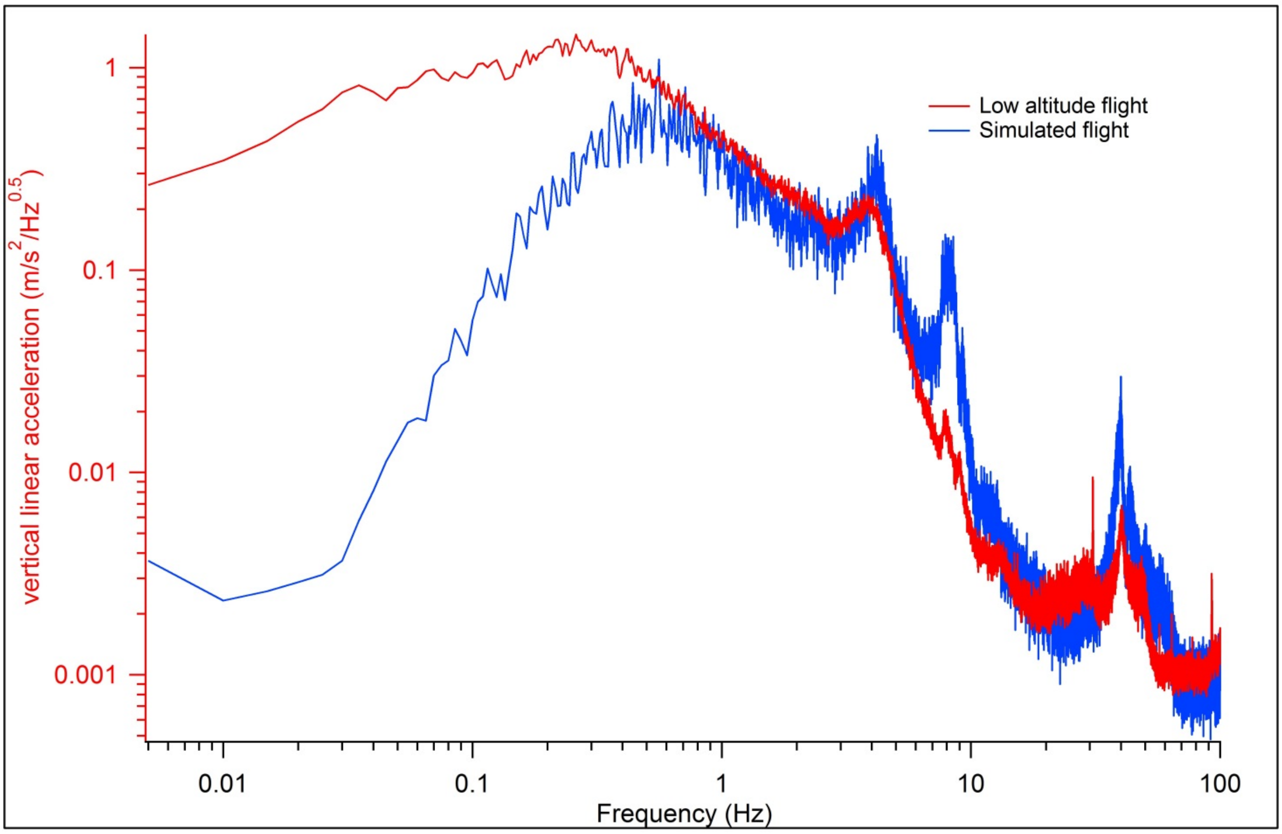

Figure 1: The power spectrum of the vertical linear acceleration of the simulated flight line, plotted with the same metric of turbulence from a real, low-altitude flight line over the R. J. Smith Airborne Gravity Test Range.

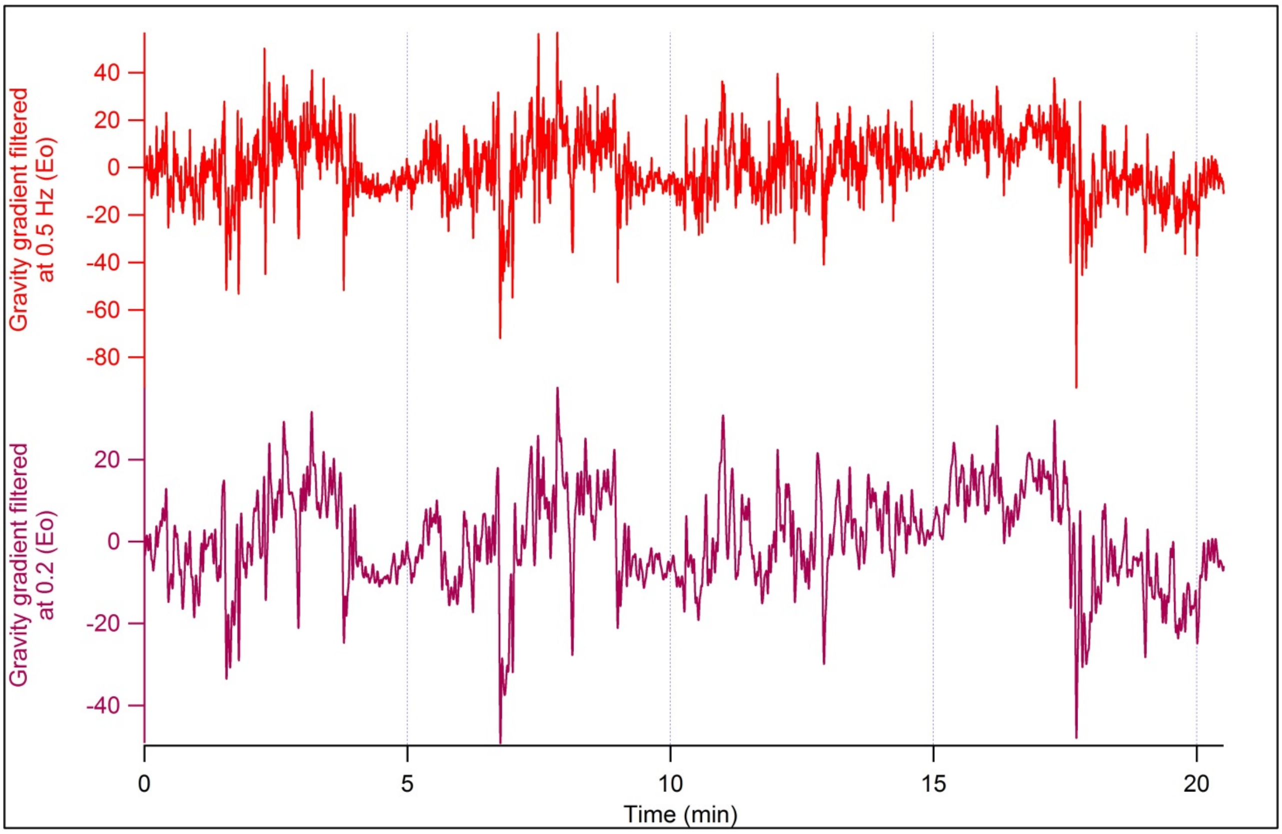

Figure 2: Top: The processed gravity gradient from four, five-minutes simulated survey flights, low pass filtered at 0.5 Hz (standard deviation = 15.2 Eö). Bottom: The same signal with a 0.2 Hz low pass filter (standard deviation = 12.3 Eö). An average flight speed of 62 m/s was simulated, resulting in a total of line 75 km.

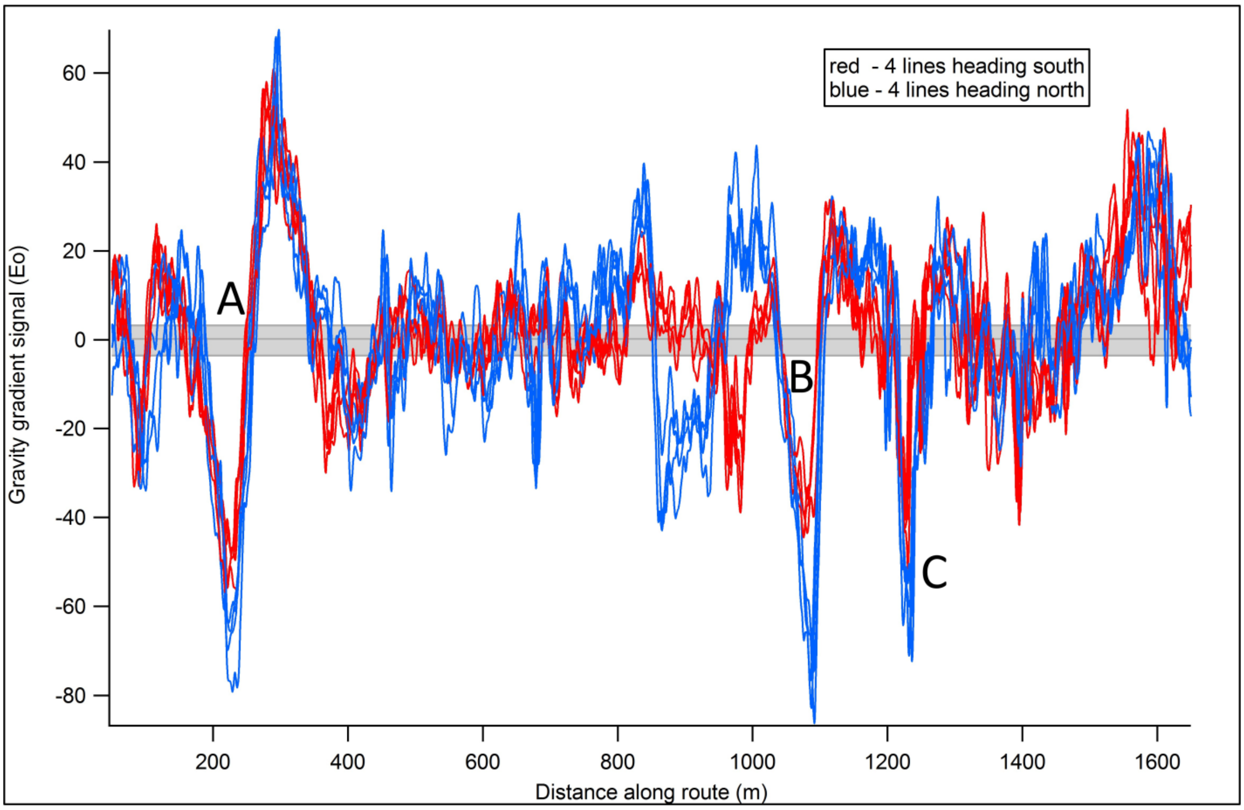

Figure 3: Processed VK1™ data for four vehicle-based trials. The data has been low-pass filtered to 0.5 Hz. The four blue profiles show data heading north along the test road, while the four red profiles show data heading south along the same road. 'A' and 'B' correspond to anomalies described in Figure 4.

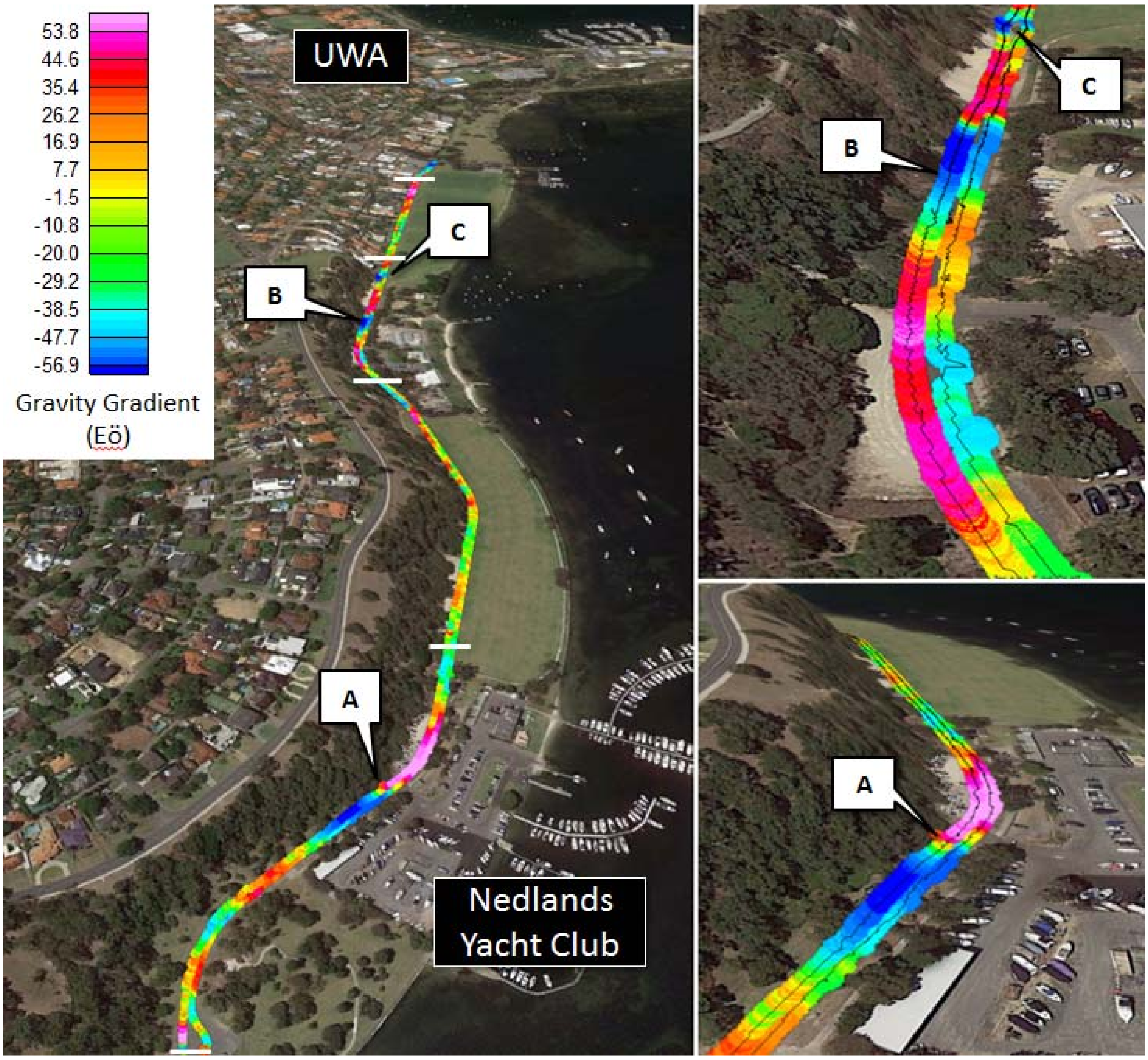

Figure 4: Left: A summary view of one van trial, showing the path that the vehicle took, with the gravity gradient along the path. Upper right: a zoomed in section of the gravity gradient in the vicinity of a road cut-out. The gravity gradient low (associated with the topographic feature) is flanked by relative gravity gradient highs. Lower right: The road-side topographic variations are evident in the recorded gravity gradient data. White lines mark 400 m segments of the road.

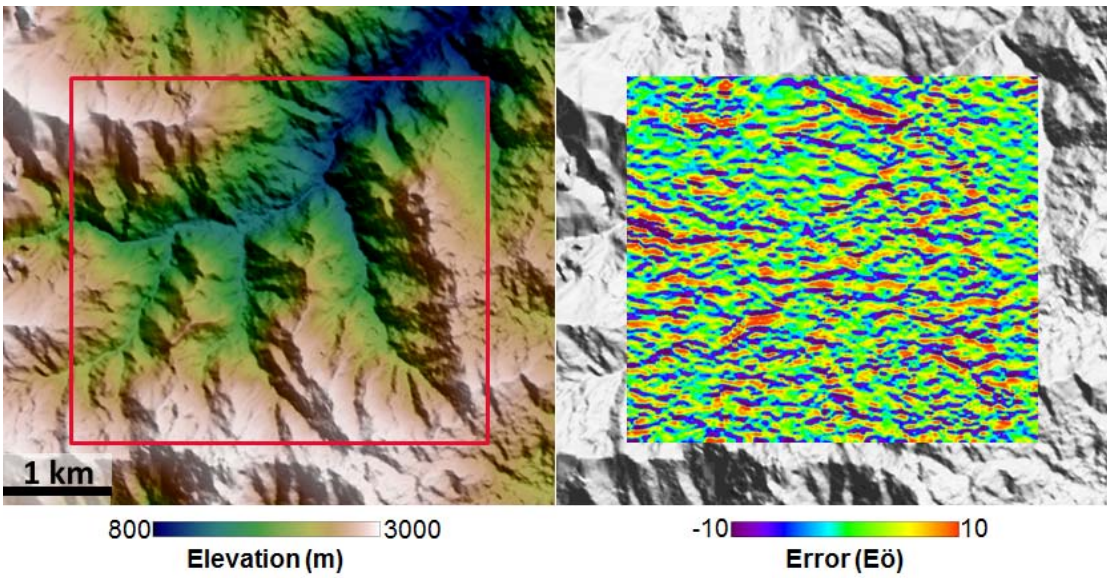

Figure 5: Left: DTM for the terrain correction spatial averaging example in the Central Andes, with the survey outline shown in red. Right: The error introduced when standard terrain corrections are applied to data that was continually acquired. This is the error caused by not applying spatial averaging.